Original Article
Anti-aging and anti-osteoporosis effects of green teen polyphenol in a premature aging model of Bmi-1 knockout mice

Yuanqing Huang[1], Li Liu[2]

[1]Department of Stomatology, Hunan University of Medicine, Huaihua 418000, Hunan, China; [2]School of Nursing, Hunan University of Medicine, Huaihua 418000, Hunan, China

Abstract: To determine whether green teen polyphenol (GTP) ameliorated the premature senescent and osteoporosis phenotype of Bmi-1$^{-/-}$ mice, we paired with littermates Bmi-1$^{+/-}$ between male and female mice, taken from the littermate mice. In vivo, the mice were divided into 3 groups and treated as following: 1) wild type (WT) mice with normal diet; 2) Bmi1$^{-/-}$ (BKO) mice with normal diet; 3) Bmi1$^{-/-}$ mice with GTP-supplemented diet (BKO+GTP) (400 mg/kg body weight/day in the drinking water). Analysis of their phenotypic differences from the whole, X-ray, morphology, protein, histochemistry and cell biology respectively, to elucidate the roles and mechanisms of GTP in premature aging and osteoporosis phenotype of Bmi-1$^{-/-}$ mice. Our results demonstrated that Bmi-1 deficiency resulted in growth retardation, premature aging and osteoporosis. We also demonstrated that these typical aging and osteoporosis phenotypes in Bmi-1-deficient mice were largely rescued by GTP through increased proliferation and decreased apoptosis, promoted skeletal growth and development, increased osteoblastic bone formation, decreased osteoclastic bone resorption and senescence-associated molecules, down-regulating oxidative stress of multiple organs, expressing antioxidase in Bmi-1$^{-/-}$ mice. These findings implied that green tea will be a novel therapeutic way to delay aging and prevent aging-associated osteoporosis.

Keywords: Green teen polyphenol, Bmi-1, aging, oxidative stress, osteoporosis

Introduction

Aging is an inevitable physiological change. It is a multifactorial process characterized by a progressive loss of physiological integrity that leads to impaired function and increased vulnerability to death [1]. Hallmarks of senescent cells include cellular DNA damage, mitochondrial dysfunction leading to increased reactive oxygen species (ROS) and decreased ATP, the production of proinflammatory cytokines, telomere shortening, the trigger of stem cell depletion and cell senescense [2]. As a representative and primary theory about senescence, the oxygen free radical hypothesis proposes that ROS attack cellular components and initiate and promote aging-associated degenerative diseases [3, 4]. Oxidative stress damages cells, tissues and organs by causing imbalance between ROS generation and antioxidant defense, contributing to the aging process [5].

Superoxide dismutase and catalase are key antioxidant enzymes that reduce O_2^- to H_2O_2 and water, delaying aging [6].

Osteoporosis, a degenerative skeletal disorder, is characterized by low bone mass and microarchitectural deterioration of bone tissue that results in compromised bone strength and increased risk of fractures [7]. Among different types of fractures, hip fracture is the most severe consequence of osteoporosis, leading to reduced activities of daily living, lowered quality of life, and increased mortality [8]. As the population ages worldwide, the increased life expectancy is accompanied with a higher prevalence of osteoporosis in the elderly population, such that osteoporosis has become a serious health concern in many countries [8, 9]. For example, in the United States, it is estimated that by 2020, there will be 61 million women and men aged 50 affected by osteoporosis or low bone

mass [3]; by 2025, the cost of osteoporosis-related expenses is projected to increase to $25.3 billion [10].

B cell-specific Moloney MLV insertion site-1 (Bmi-1) belongs to the polycomb group (PcG) genes, which are transcriptional repressors that are essential for the maintenance of appropriate gene expression patterns during development [11] is involved in cell cycle regulation, self-renewal of stem cells and cell senescence [12, 13]. It is well established that not only deletion of Bmi-1 prematurely produces a typical osteoporotic phenotype, but also Bmi-1$^{-/-}$ mice exhibit a total body premature aging phenotype [13]. Protection against oxidative stress and apoptosis emerges as an important Bmi1-downstream pathway as well, either by reducing P53 levels via Bmi-1-mediated repression of the INK4a/Arf locus or via modulation of the oxidative stress response in an INK4a/Arf-independent manner. In Bmi1$^{-/-}$ mice, the increase in ROS coincided with an increase in DNA damage and an activation of the DNA damage repair pathways, and treatment with NAC or targeting of CHK2 at least partially restored some of the phenotypes [14].

Tea, the dried leaves of the plant Camellia sinensis species of the Theaceae family, is one of the most widely consumed beverages in the world with a production of 4.52 million tons in 2010, including black tea (78%) in Western countries, green tea (20%) in Asian countries, and oolong tea (2%) in southern China [15]. Tea is an important source of dietary flavonoids, especially flavanols, and it has been associated with protecting against bone loss and reducing risk of fractures.

Evidence from these in vitro studies suggests that tea polyphenolsmay benefit bone health by enhancing osteoblastogenesis and suppressing osteoclastogenesis through modulation of growth factors, cytokines, and chemokines and their receptors Theaflavins are the major polyphenols in black tea and are composed principally of theaflavin, theaflavin-3-gallate, theaflavin-3'-gallate, and theaflavin-3, 3'-gallate [16]. Oka et al recently showed that theaflavin-3, 3-gallate inhibits the formation and differentiation of osteoclasts via suppression of matrix metalloproteinases [17].

Compared with black tea, there are many more studies showing a positive impact of green tea

on bone health. Green tea polyphenol (GTP), including epigallocatechin-3-gallate (EGCG; the most abundant polyphenol in green tea), epigallocatechin, epicatechin-3-gallate (ECG), epicatechin, and catechins [18]. In vitro studies have shown the antiresorptive properties of green tea's bioactive components through increasing apoptosis of osteoclasts, suppression of osteoclast formation, and inhibition of bone re-sorption. For instance, EGCG enhances osteoclastic cell death through the Fenton reaction and caspase-3 activation [19, 20]. EGCG suppresses osteoclast formation by inhibiting the expression of matrix metalloproteinase-9 in osteoblasts [17, 21]. EGCG inhibits bone resorption via inhibition of IL-6 production or suppression of p44/p42 MAP kinase activation [22, 23]. EGCG sup-presses osteoclastic differentiation via downregulation of the receptor activator of NF-κB ligand (RANKL)-induced expression of the nuclear transcription factor of activated T cells c1, thus blocking differentiation of monocytes into osteoclasts, followed by decreased bone resorption [24, 25]. EGCG has also been shown to block RANKL signaling by suppressing RANKL-induced NF-κB transcription activity, a pathway essential to osteoclastogenesis [26].

Green tea's bioactive components have also been shown to benefit osteoblastogenesis by increasing osteoblastic survival, proliferation, differentiation, and mineralization. Observations from in vitro studies support such stimulatory effects of EGCG on osteoblastogenesis. However, it is unclear whether green teen delay aging and prevent aging-associated degenerative diseases by migrating into organs and maintaining redox balance.

To investigate the potential of green tea, in the present study, we utilize Bmi-1 knockout mice induced typical premature senescent and osteoporosis phenotype. We hypothesize whether green tea could rescue deletion of Bmi-1 induced the phenotype premature senescence and osteoporosis through anti-oxidative stress pathway.

Materials and methods

Mice and genotyping

The Bmi-1 heterozygote (Bmi-1$^{+/-}$) mice (129Ola/FVB/N hybrid back-ground) were backcrossed 10-12 times to the C57BL/6J background and mated to generate Bmi-1 homozygote (Bmi-1$^{-/-}$)

and their wild-type (WT) littermates genotyped by PCR, as described previously [13, 27]. Mice were maintained in the Experimental Animal Center of Nanjing Medical University. This study was carried out in strict accordance with the guidelines of the Institute for Laboratory Animal Research of Nanjing Medical University. The protocol was approved by the Committee on the Ethics of Animal Experiments of Nanjing Medical University.

Animals treatment and supplementary of green tea polyphenol (GTP)

Purified GTP was made in Golden Green Biological Technology Co., Ltd., Xian, China. In vivo, animals were divided into 3 groups of 6 mice each and treated as following:

1) Normal diet (WT) group: 3-week weaning littermate wild type mice were fed normal diet for 4 weeks. 2) Normal diet (BKO) group: 3-week weaning littermate Bmi-1 knockout mice were fed normal diet for 4 weeks. 3) Supplementation of GTP (BKO+GTP) group: 3-week weaning littermate Bmi-1 knockout mice were fed Supplementation of GTP (400 mg/kg body weight/day in the drinking water) for 4 weeks [28]. Seven weeks later, 3 groups of 6 mice each were sacrificed for further analysis.

Analysis of mice phenotype, percent survival, and body weight

In order to investigate the effect of GTP on Bmi-1$^{-/-}$ mice total body, In vivo, other animals were divided into 3 groups of 6 mice (WT, BKO, BKO+GTP). We carried out statistic analysis of phenotype, body weight, and percent survival in different groups mice respectively.

Radiography

Tibiae were removed and dissected free of soft tissue. Contact radiographs were taken using a Faxitron model 805 radiographic inspection system (Faxitron Contact, Faxitron, Ethican, Norderstedt, Germany) (22 kV voltage and 4 min exposure time). X-Omat TL film (Eastman Kodak Co.) was used and processed routinely.

Histology

Tibiae were removed and fixed in PLP fixative (2% paraformaldehyde containing 0.075 M lysine and 0.01 M sodium periodate) overnight at 4°C, and processed histologically as described [29]. Proximal ends of tibiae were decalcified in EDTA glycerol solution for 5-7 days at 4°C. Decalcified samples were dehydrated and embedded in paraffin, and 5 μm sections were cut on a rotary microtome. The sections were stained with Hematoxylin and Eosin (HE), or histochemically for total collagen (TCOL), alkaline phosphatase (ALP) activity or tartrate-resistant acid phosphatase (TRAP), or immunohistochemically as described below.

Histochemical staining for collagen, ALP and TRAP

Total collagen was detected in paraffin-embedded sections using a modified method of Lopez-De Leon and Rojkind [30]. Dewaxed sections were exposed to 1% Sirius Red in saturated picric acid for 1 hour. After washing with distilled water, the sections were counterstained with Hematoxylin and mounted with Biomount medium (Canemco, Quebec, Canada).

Enzyme histochemistry for ALP activity was performed as described [31]. Briefly, following pre-incubation overnight in 100 mM MgCl$_2$ in 100 mM Tris-maleate buffer (pH 9.2), dewaxed sections were incubated for 2 hours at room temperature in 100 mM Tris-maleate buffer containing naphthol AS-MX phosphate (0.2 mg/ml, dissolved in ethylene glycol monomethyl ether, both Sigma) as substrate and Fast Red TR (0.4 mg/ml, Sigma) as a stain for the reaction product. After washing with distilled water, the sections were counterstained with Vector Methyl Green nuclear counterstain (Vector Laboratories, Burlington, Ontario, Canada) and mounted with Kaiser's glycerol jelly.

Enzyme histochemistry for TRAP was performed using a modification of a previously described protocol [32]. Dewaxed sections were preincubated for 20 minutes in buffer containing 50 mM sodium acetate and 40 mM sodium tartrate (pH 5.0). Sections were then incubated for 15 minutes at room temperature in the same buffer containing 2.5 mg/ml naphthol AS-MX phosphate in dimethylformamide as substrate and 0.5 mg/ml Fast Garnet GBC (Sigma) as a color indicator for the reaction product. After washing with distilled water, the sections were counterstained with Methyl Green and mounted in Kaiser's glycerol jelly.

β-gal staining and immunohistochemical staining

Pre-embedding senescence-associated-b-gal (SA-b-gal), was performed following previously described methods [33]. Immunohistochemical staining was carried out for type I collagen (I-COL) using the avidin-biotin-peroxidase complex technique with affinity-purified goat anti-rabbit I-COL antibody (Southern Biotech, Birmingham, AL, USA) as described previously [33]. Briefly, dewaxed and rehydrate paraffin-embedded sections were incubated with methanol-hydrogen peroxide (1:10) to block endogenous peroxidase activity and then washed in Tris-buffered saline (pH 7.6). The slides were then incubated with the primary antibodies overnight at room temperature. After rinsing with Tris-buffered saline for 15 min, sections were incubated with biotinylated secondary antibody (Sigma, St. Louis, MO, USA). Sections were then washed and incubated with the Vectastain Elite ABC reagent (Vector Laboratories, Burlington, Canada) for 45 min. After washing, brown pigmentation was likewise produced using 3,3-diaminobenzidine (DAB). Finally, the stained sections were counterstained with H&E staining. Images were acquired with a Leica microscope (Leica DM4000B, Solms, German) equipped with Leica software.

Quantitative real-time PCR

RNA was isolated from mouse tibiae using Trizol reagent (Invitrogen, CA, USA) according to the manufacturer's protocol. Reverse transcription reactions were performed using the SuperScript First-Strand Synthesis System (Invitrogen, CA, USA) as described [34]. To determine the number of cDNA molecules in the reverse-transcribed samples, real-time PCR analyses were performed using the LightCycler system (Roche, Indianapolis, IN, USA). PCR was performed using 2 µL Light-Cycler DNA Master SYBR Green I (Roche, Indianapolis, IN, USA), 12.5 µL of reaction mixture, 2 µL of each 5' and 3' primer, 2 µL samples and then H_2O was added to a final volume of 25 µL. Samples were denatured at 95°C for 10 seconds, with a temperature transition rate of 20°C per sec. Amplification and fluorescence determination were carried out in four steps: denaturation at 95°C for 1 second, with a temperature transition rate of 20°C/sec; annealing for 5 seconds, with a temperature transition rate of 8°C/sec; extension at 72°C for 20 seconds, with a temperature transition rate of 4°C/sec; and detection of SYBR Green fluorescence, which reflects the amount of double-stranded DNA, at 86°C for 3 seconds. The amplification cycle number was 35. To discriminate specific from nonspecific cDNA products, a melting curve was obtained at the end of each run. Products were denatured at 95°C for 3 seconds, and the temperature was then decreased to 58°C for 15 seconds and raised slowly from 58 to 95°C using a temperature transition rate of 0.1°C/sec. To determine the number of copies of the targeted DNA in the samples, purified PCR fragments of known concentrations were serially diluted and served as external standards that were measured in each experiment. Data were normalized with GAPDH levels in the samples. The primer sequences used for the real-time PCR were as described [35].

Western blot analysis

Proteins were extracted from femur, lung, spleen, skin and quantitated by a kit (Bio-Rad, Mississauga, Ontario, Canada). Protein samples were fractionated by SDS-PAGE and transferred to nitro-cellulose membranes. Western blot was carried out as described previously [35] using antibodies against RunX2 (goat anti-mouse, M-156, Santa Cruz Biotechnology, USA), Sirt1 (goat anti-mouse, Santa Cruz Biotechnology, USA), Prdx1 (goat anti-rabbit, Abcam, UK), SOD1 (goat anti-rabbit, Abcam, UK), p53 (goat anti-mouse, Cell Signal, China), Bcl-2 (goat anti-rabbit, Abcam, UK), PTEN and Caspase-3 (goat anti-mouse, Santa Cruz, CA, USA), and actin (goat anti-rabbit, Santa Cruz Biotechnology, USA). Bands were visualized using enhanced chemiluminescence (ECL, Amersham) and quantitated by Scion Image Beta 4.02 (Scion Corporation, Bethesda, MD, USA).

Computer-assisted image analysis

After H&E staining or histochemical or immunohistochemical staining of sections from 3 groups of 6 mice each, images of interested fields were photographed with a SONY digital camera. Images of micrographs from single section were digitally recorded using a rectangular template, and recordings were processed and analyzed using Northern Eclipse image analysis software as described previously [13].
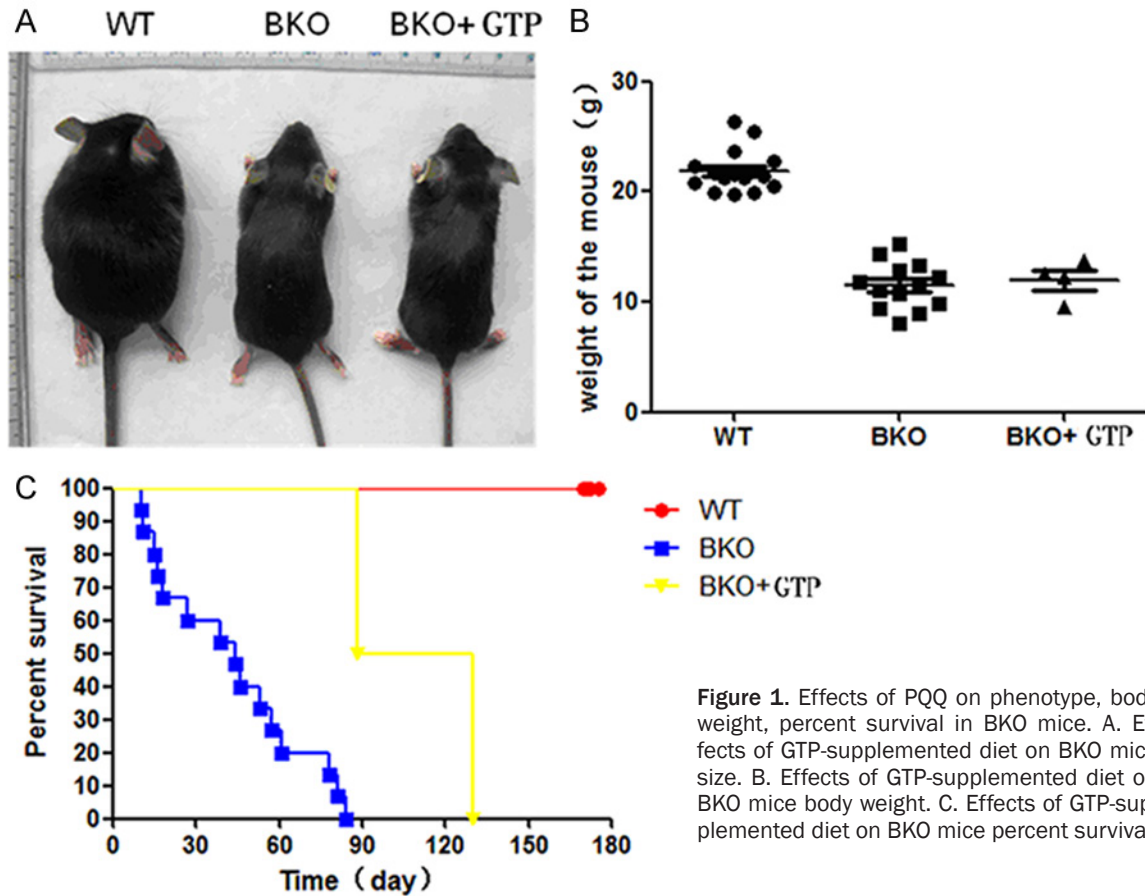
Figure 1. Effects of PQQ on phenotype, body weight, percent survival in BKO mice. A. Effects of GTP-supplemented diet on BKO mice size. B. Effects of GTP-supplemented diet on BKO mice body weight. C. Effects of GTP-supplemented diet on BKO mice percent survival.

Statistic analysis

All data were expressed as mean ± standard error. Statistical analysis of numeration data were performed using analysis of χ^2 text, while statistical analyses of measurement data were performed using analysis of student's t-test. The significance level was set at P<0.05.

Results

Effects of GTP on premature aging phenotype in Bmi-1$^{-/-}$ mice

To investigate whether GTP-supplemented diet could rescue Bmi-1$^{-/-}$ mice premature aging phenotype, we performed statistic analysis of phenotype, body weight, and percent survival in different groups mice respectively. As shown in **Figure 1A-C**, compared with normal diet feeding only (WT) mice, BKO mice with normal diet significantly showed a premature aging phenotype, body weight loss, and shortened percent survival. Whereas BKO mice with GTP-supplemented diet didn't rescue total body size

body weight, however, prolonged percent survival compared to BKO mice with normal diet. These data support that GTP-supplemented diet could significantly prolong percent survival in Bmi-1$^{-/-}$ mice compared with normal diet.

Effects of GTP on tibiae growth and development, osteoblastic bone formation and osteoclastic bone resorption in Bmi-1$^{-/-}$ mice

To assess the effect of GTP on postnatal skeletal growth and development, osteoblastic bone formation and osteoclastic bone resorption in Bmi-1$^{-/-}$ mice, long bones were analyzed at 7 weeks of ages by radiography (**Figure 2A**). The lengths of femurs were shorter in Bmi-1$^{-/-}$ mice than in their wild-type littermates , but longer in the BKO+GTP mice than in Bmi-1$^{-/-}$ mice (see **Figure 2A**). Radiolucency was greater in BKO+GTP mice relative to Bmi-1$^{-/-}$ mice (see **Figure 2A**). Consistent with radiography analysis, histologic analysis of TCOL demonstrated that trabecular bone volume was reduced significantly in Bmi-1$^{-/-}$ mice compared with their wild-type littermates, however increased signif-
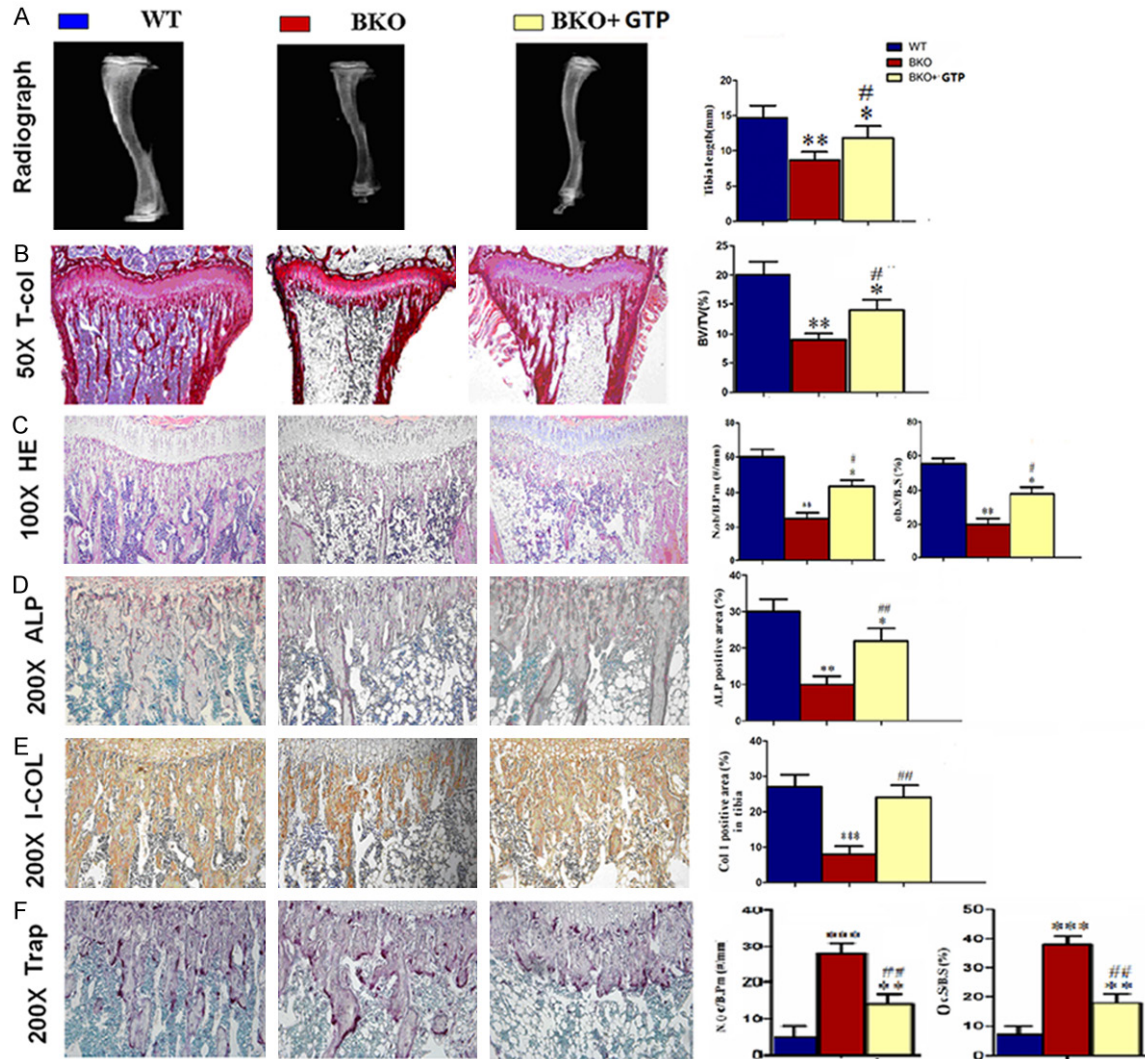
Figure 2. Effects of GTP on tibiae growth and development, osteoblastic bone formation and osteoclastic bone resorption in Bmi-1$^{-/-}$ mice. A. Representative contact radiographs of the femurs of wild-type (WT), Bmi-1$^{-/-}$ mice (BKO) and BKO+GTP mice; B. Representative micrographs of the proximal ends of tibiae from WT, BKO and BKO+GTP mice stained histochemically for total collagen; C. Representative micrographs of tibial sections from WT, BKO and BKO+GTP mice stained with H&E; D. Representative micrographs of tibial sections from WT, BKO and BKO+GTP mice stained histochemically for alkaline phosphatase (ALP); E. Representative micrographs of tibial sections from WT, BKO and BKO+GTP mice stained with immunostained for type I collagen (Col I); F. Representative micrographs of tibial sections from WT, BKO and BKO+GTP mice stained histochemically for tartrate-resistant acid phosphatase activity (TRAP). Each value is the mean ± SEM of determinations in six animals of the same groups. *, P<0.05; **, P<0.01; ***, P<0.001, compared with WT mice; #, P<0.05; ##, P<0.01; ###, P<0.001, compared with BKO mice. Number of positive osteoblasts (N.Ob/B.Pm (#/mm). Percent ratio of positive areas osteoblasts (Ob.S/B.S (%)). Number of TRAP-positive osteoclasts (N.Oc/B.Pm, #/mm). Surface of TRAP-positive osteoclasts (Oc.S/B.S, %).

icantly in the BKO+GTP mice than in Bmi-1$^{-/-}$ mice (see **Figure 2B**). These results indicate that GTP could partially rescue skeletal growth retardation and premature osteoporosis. To determine whether GTP rescued the phenotype of premature osteoporosis associated with osteoblastic bone formation and osteoclastic bone resorption, the number of osteoblasts, ALP activity in osteoblasts, type I collagen

deposition in bone matrix, and TRAP activity in osteoclasts were examined by H&E staining (**Figure 2C**), histochemical staining for ALP (**Figure 2D**), immunostaining for type I collagen (**Figure 2E**), and histochemical staining for TRAP (**Figure 2F**), respectively. The number of osteoblasts, ALP and type I collagen positive area in the metaphyeal region, in both endosteum and trabeculae were increased signifi-
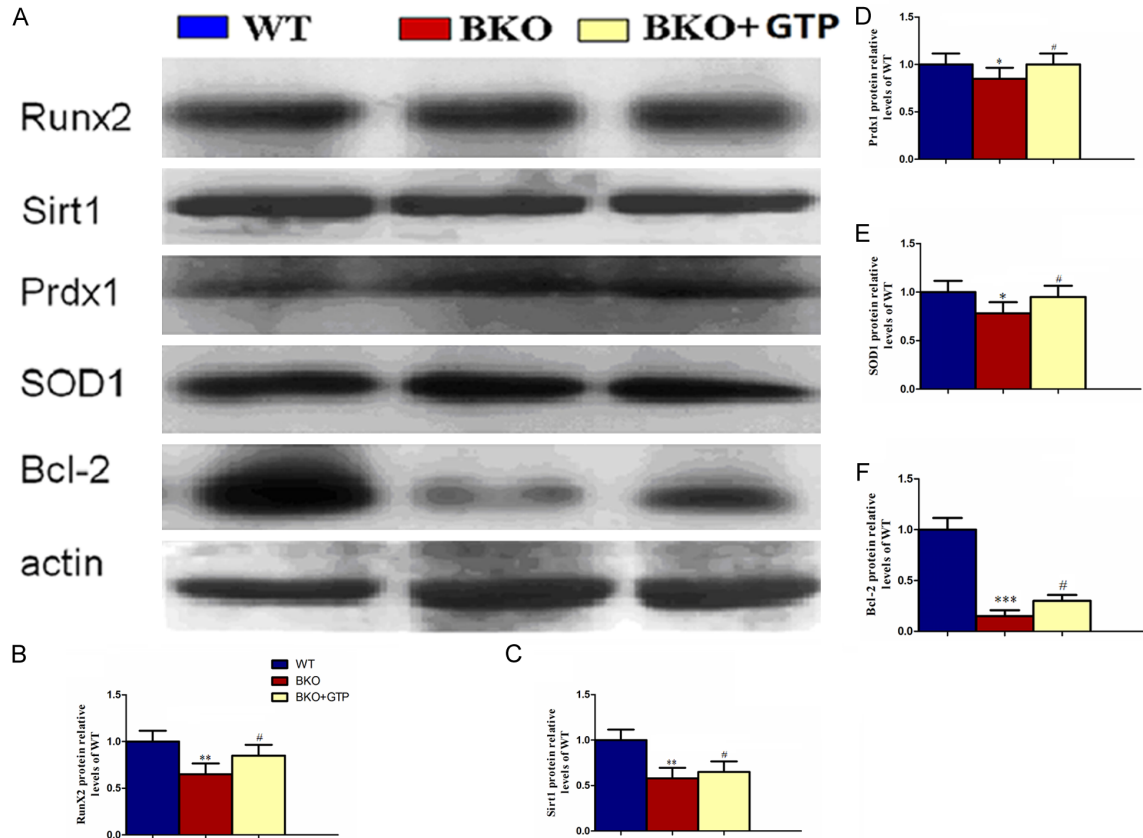
Figure 3. *Effects of GTP on the expression of antioxidant proteins in Bmi-1$^{-/-}$ mice.* (A) Western blots of femur extracts from wild-type (WT), Bmi-1$^{-/-}$ mice (BKO) and BKO+GTP mice for expression of Runx2, Sirt1, Prdx1, SOD1, Bcl-2. actin was used as loading control for Western blots. (B) Runx2, (C) Sirt1, (D) Prdx1, (E) SOD1 and (F) Bcl-2 protein levels relative to actin level were assessed by densitometric analysis and expressed relative to levels of WT and BKO mice. Each value is the mean ± SEM of determinations in six animals of the same genotype. *, P<0.05; **, P<0.01; ***, P<0.001, compared with WT mice; #, P<0.05; ##, P<0.01; ###, P<0.001, compared with BKO mice.
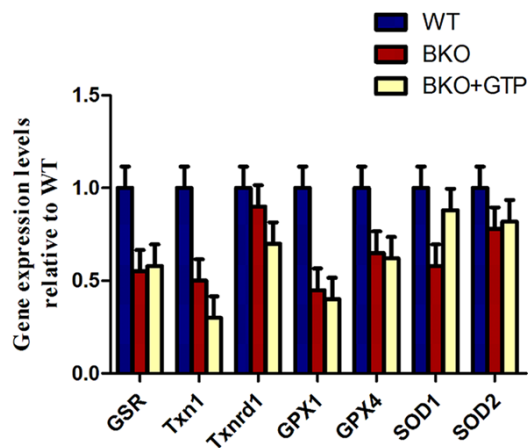

Figure 4. Effects of GTP on oxidative stress related genes in Bmi-1$^{-/-}$ mice. Glutathione reductase (GSR), Txn1, Txnrd1, Glutathione peroxidase 1 (Gpx1), GPX4, SOD1 and SOD2 mRNA relative levels in humerus demonstrated by real-time RT-PCR, calculated as a ratio to GAPDH mRNA, expressed relative to WT.

cantly in BKO+GTP mice than in Bmi-1$^{-/-}$ mice (see **Figure 2A-E**). However, the number of osteoclasts were decreased significantly in BKO+GTP mice than in Bmi-1$^{-/-}$ mice (see **Figure 2F**). The results indicated that GTP partially rescued premature osteoporosis associated with osteoblastic bone formation and osteoclastic bone resorption.

Effects of GTP on the expression of femur antioxidant proteins in Bmi-1$^{-/-}$ mice

To determine whether GTP increased osteoblasts and decreased osteoclasts associated with alterations of Runx2, Sirt1, Prdx1, SOD1 and Bcl-2 expression, respectively. Proteins were isolated from femur, and Western blots were performed (see **Figure 3A**). Results showed that the expression levels of Runx2, Sirt1, Prdx1, SOD1 and Bcl-2 were all up-regulated (see **Figure 3B-F**). From the above results,
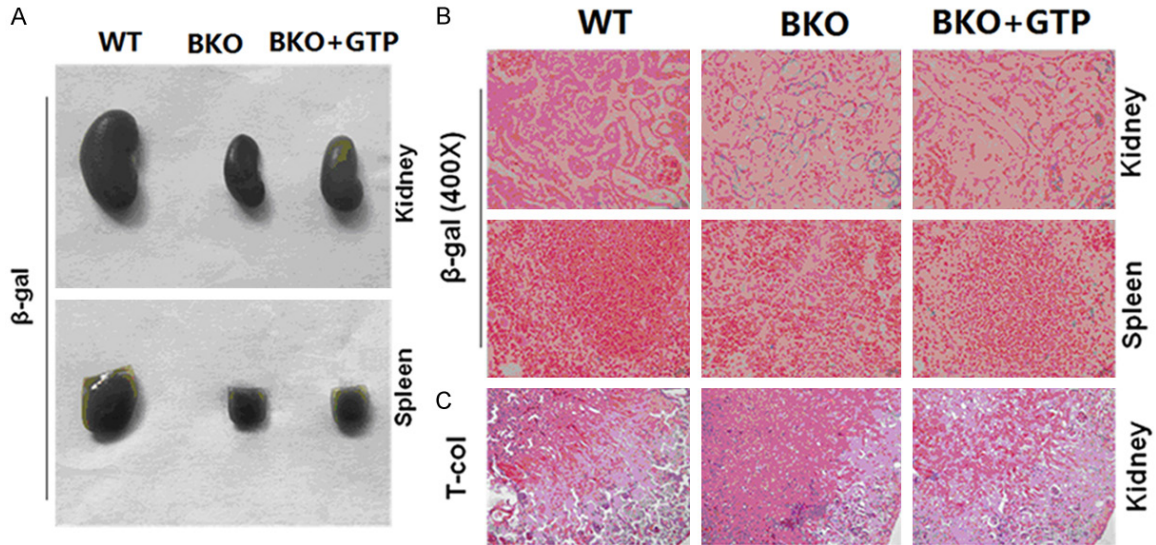
Figure 5. Bmi-1 deficient-induced proapoptosis and aging were ameliorated by GTP treatment in Bmi-1$^{-/-}$ mice. A and B. Senescence-associated-b-galactosidase (SA-b-gal) of kidney and spleen in wild-type (WT), Bmi-1$^{-/-}$ mice (BKO) and BKO+GTP mice; C. Representative micrographs of kidney from WT, BKO and BKO+GTP mice stained histochemically for total collagen.

we found that the core transcription factor Runx2, bone marrow mesenchymal stem cells, a key gene for bone formation, was necessary to bone differentiation and bone development. Sirt1, promoted osteoblast differentiation gene, Prdx1, peroxidase gene, superoxide dismutase (SOD1) and antiapoptotic gene Bcl-2 after giving GTP have a tendency to increase. The results indicated that GTP could play bone formation and antioxidant roles in Bmi-1$^{-/-}$ mice.

Effects of GTP on oxidative stress related genes in Bmi-1$^{-/-}$ mice

To determine whether GTP increased osteoblasts and decreased osteoclasts associated with alterations of GSR, Txn1, Txnrd1, Gpx1, GPX4, SOD1 and SOD2 mRNA relative levels expression, respectively. RNA were extracted from humerus, and real-time RT-PCR were performed (see **Figure 4**). From the above results, we found that supplementation of GTP increased GSR, SOD1 and SOD2 mRNA relative levels. The results showed that GTP rescued *Bmi-1$^{-/-}$* mice bone phenotypes through up-regulating some antioxidant gene.

Effects of GTP on Bmi-1 deficient-induced pro-apoptosis and aging in Bmi-1$^{-/-}$ mice

To determine whether *GTP* ameliorated Bmi-1 deficient-induced proapoptosis and aging, kid-

ney and spleen were analyzed at 7 weeks of ages by SA-b-gal and stained histochemically for total collagen (see **Figure 5A-C**). From the above results, GTP reduced age-related beta galactose glucoside enzyme positive areas from kidney and spleen compared to BKO mice. T-col positive areas was reduced in kidney and renal fibrosis was reduced in BKO+GTP mice. This results showed that GTP played anti-aging roles of kidney and spleen in Bmi-1$^{-/-}$ mice.

Effects of GTP on proliferation, aging and apoptosis of lung in Bmi-1$^{-/-}$ mice

To determine whether GTP played proliferation, anti-aging and anti-apoptosis of lung in wild-type (WT), Bmi-1$^{-/-}$ mice (BKO) and BKO+GTP mice, Proteins were isolated from lung at 7 weeks of ages, and Western blots were performed (see **Figure 6A**). Results showed that the expression levels of PTEN and Bcl-2 were up-regulated, however, p53 was down-regulated (see **Figure 6B-D**). The results showed that GTP played anti-apoptosis and anti-aging roles of lung in Bmi-1$^{-/-}$ mice.

Effects of GTP on proliferation, apoptosis and aging of speen in Bmi-1$^{-/-}$ mice

To determine whether GTP played proliferation, anti-apoptosis and anti-aging of speen in wild-type (WT)*,* Bmi-1$^{-/-}$ mice (BKO) and BKO+GTP mice, Proteins were isolated from speen at 7
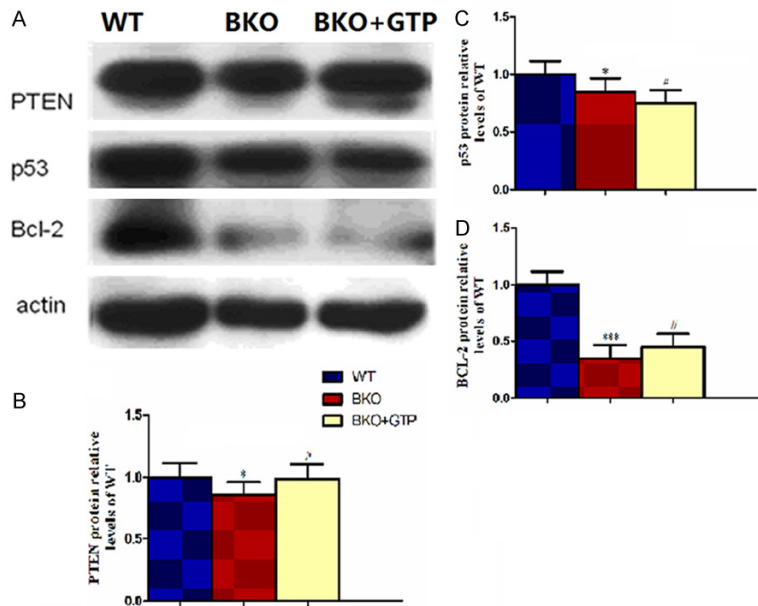
Figure 6. Effects of GTP on proliferation, aging and apoptosis of lung in Bmi-1$^{-/-}$ mice. (A) Western blots of lung extracts from wild-type (WT), Bmi-1$^{-/-}$ mice (BKO) and BKO+GTP mice for expression of PTEN, p53, Bcl-2. actin was used as loading control for Western blots. (B) PTEN, (C) p53, (D) Bcl-2 protein levels relative to actin level were assessed by densitometric analysis and expressed relative to levels of WT and BKO mice. Each value is the mean ± SEM of determinations in six animals of the same genotype. *, P<0.05; **, P<0.01; ***, P<0.001, compared with WT mice; #, P<0.05; ##, P<0.01; ###, P<0.001, compared with BKO mice.

weeks of ages, and Western blots were performed (see **Figure 7A**). Results showed that the expression level of Bcl-2 were up-regulated, however, PTEN and caspase3 were down-regulated (see **Figure 7B-D**). The results showed that GTP partially played anti-apoptosis and anti-aging roles of speen in Bmi-1$^{-/-}$ mice.

Effects of GTP on the expression of antioxidant proteins of skin in Bmi-1$^{-/-}$ mice

To determine whether GTP prolonged skin aging associated with alterations of SOD1 and Bcl-2 expression, respectively. Proteins were isolated from skin, and Western blots were performed (see **Figure 8A**). Results showed that the expression levels of SOD1 and Bcl-2 were all up-regulated (see **Figure 8B**, **8C**). From the above results, we found that peroxidase gene, superoxide dismutase (SOD1) and antiapoptotic gene Bcl-2 after giving GTP have a tendency to increase. The results showed that GTP partially played anti-apoptosis and anti-aging roles of skin by up-regulating antioxidant ability in Bmi-1$^{-/-}$ mice.

Discussion

Osteoporosis is the result of an imbalance in the ratio with more resorption than formation. Enhancing the activity of osteoblasts, plus reducing that of the osteoclasts, may help restore the balance in bone metabolism and limit bone loss in the development of osteoporosis. There is mounting evidence that green tea contains many bioactive ingredients that support some protection against osteoporosis. This is supported by data from in vitro, ex vivo, and in vivo animal studies and human epidemiological findings. The beneficial effects of tea bioactive products seem to be mediated through anti-oxidant or anti-inflammatory pathways and their related signaling pathways in the various cells that comprised bone compartments.

In this study, we demonstrated that Bmi-1 deficiency resulted in growth retardation and premature aging because of decreased proliferation and increased apoptosis, impaired skeletal growth and development and premature osteoporosis associated with decreased osteoblastic bone formation, increased osteoblastic bone resorption and up-regulated senescence-associated molecules, and increased oxidative stress and DNA damage of multiple organs. Our results also demonstrated that these typical aging and osteoporosis phenotypes in Bmi-1-deficient mice were largely rescued by green teen polyphenols (GTP) through anti-aging, anti-apoptosis, proliferating, expressing antioxidase in Bmi-1$^{-/-}$ transplant recipients. These findings indicated that GTP had preventative and therapeutic potential for aging and aging-associated degenerative diseases such as osteoporosis.

Bmi-1, derived from the polycomb family, inhibits space-specific and time-specific expression of the Hox gene in growth and development. Bmi-1 systematic deficiency leads to shortened
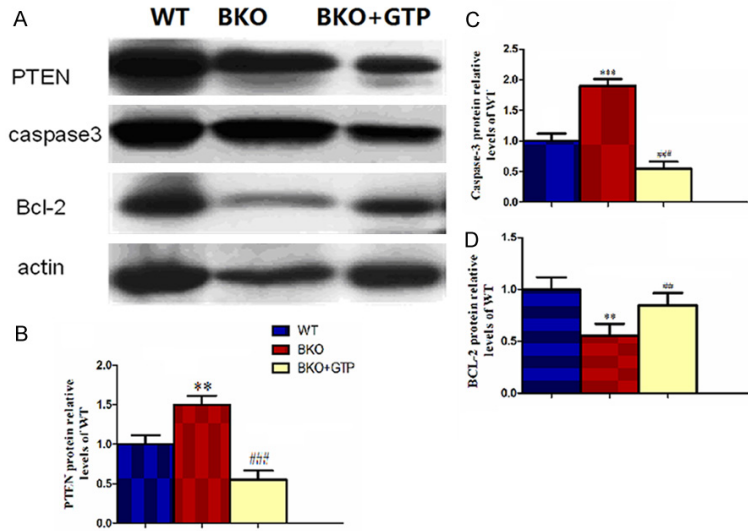
Figure 7. Effects of GTP on proliferation, apoptosis and aging of speen in Bmi-1$^{-/-}$ mice. (A) Western blots of speen extracts from wild-type (WT), Bmi-1$^{-/-}$ mice (BKO) and BKO+GTP mice for expression of PTEN, caspase3, Bcl-2. actin was used as loading control for Western blots. (B) PTEN, (C) caspase3, (D) Bcl-2 protein levels relative to actin level were assessed by densitometric analysis and expressed relative to levels of WT and BKO mice. Each value is the mean ± SEM of determinations in six animals of the same genotype. *, P<0.05; **, P<0.01; ***, P<0.001, compared with WT mice; #, P<0.05; ##, P<0.01; ###, P<0.001, compared with BKO mice.

life span and growth retardation [12, 13]. Consistent with these results, we found that Bmi-1 deficiency led to shortened survival rates, and decreased body weight and overall size of the body, spleen and kidney. We found that GTP prolonged survival, increased overall sizes of spleen and kidney directly by promoting cell proliferation and inhibiting cell apoptosis in Bmi-1 deficient mice. Thus, GTP rescued the shortened life span and growth retardation in a model of systematic senescence and osteoporosis.

Our previous results demonstrated that Bmi-1 deficiency leads to aging-associated os-teoporosis, as determined by down-regulated self-renewal capacity of bone marrow mesenchymal stem cells [13]. The study has evidence suggesting that GTP significantly slow the loss of bone density and prolong the life span of Bmi-1$^{-/-}$ mice. Results from this study indicate that GTP rescued aging-associated osteoporosis by promoting osteogenesis and inhibiting apoptosis.

Both osteoblastic and osteoclastic cells regulate bone metabolism, and both cell types are involved in the development of osteoporosis [36]. Osteoblasts are bone-forming cells located near the surface of the bone that produces cytokines. Cytokines, including macrophage colony-stimulating factor (M-CSF) and receptor activator of nuclear factorκB (NF-κB) ligand (RANKL), are both essential for osteoclast differentiation, function, and survival [37, 38]. Osteoclasts are bone-resorbing multinucleated cells that become tightly attached to mineralized bone surfaces through their integrins and form resorption lacuna by secreting protons, proteases, and superoxide through ruffled borders [39-42]. Bone resorption by activated osteoclasts with subsequent deposition of a new matrix by osteoblasts causes the formation of bone structure and bone remodeling [36]. Imbalance between bone formation and bone resorption is the key pathophysiological event in many metabolic bone disorders in adult humans, including osteoporosis, a result of bone loss [43].

Oxidative stress is a pivotal pathogenic factor for age-related bone loss inmice and rats [44-46], leading to an increase in osteoblast and osteocyte apoptosis, among other changes, and a decrease in osteoblast numbers and the rate of bone formation via Wnt/β-catenin signaling [45]. Recent studies showed that oxidative stress inhibited osteoblastic differentiation [47, 48] via extracellular signal-regulated kinases (ERKs) and ERK-dependent NF-κB signaling pathways [49]. Osteoblasts can produce antioxidants, such as glutathione peroxidase, to protect against reactive oxygen species (ROS) [50], as well as transforming growth factor β (TGF-β), which is involved in a reduction of bone resorption [51]. Reactive oxygen species are also involved in bone resorption with a direct contribution of osteoclast-generated superoxide to bone degradation, and oxidative stress increases differentiation and function of osteoclasts [52-54].
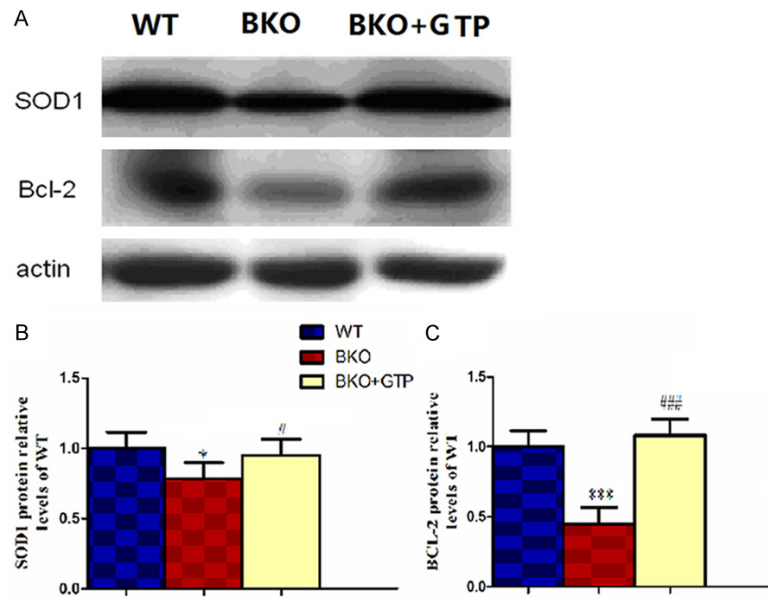
Figure 8. Effects of GTP on the expression of antioxidant proteins of skin in Bmi-1$^{-/-}$ mice. (A) Western blots of skin extracts from wild-type (WT), Bmi-1$^{-/-}$ mice (BKO) and BKO+GTP mice for expression of SOD1 and Bcl-2. actin was used as loading control for Western blots. (B) SOD1, (C) Bcl-2 protein levels relative to actin level were assessed by densitometric analysis and expressed relative to levels of WT and BKO mice. Each value is the mean ± SEM of determinations in six animals of the same genotype. *, P<0.05; **, P<0.01; ***, P<0.001, compared with WT mice; #, P<0.05; ##, P<0.01; ###, P<0.001, compared with BKO mice.

efits in treating osteoporosis.

In conclusion, GTP could express anti-oxidase, promote growth and delay senescence by stimulating proliferation and inhibiting apoptosis; ameliorate impaired skeletal growth and development and premature osteoporosis by promoting osteogenesis, inhibiting apoptosis and down-regulating senescence-associated molecules; inhibit oxidative stress and DNA damage of multiple organs in Bmi-1$^{-/-}$ mice. Results from this study indicate that green tea ameliorated the premature senescent phenotype of Bmi-1 deficient mice. Our findings implied that green tea will be a novel therapeutic way to delay aging and prevent aging-associated osteoporosis.

Disclosure of conflict of interest

None.

Address correspondence to: Dr. Yuanqing Huang, Department of Stomatology, Hunan University of Medicine, No. 492, Jinxi South Road, Huaihua 418-000, Hunan, China. E-mail: huang1977789@126.com

In the study, these significant beneficial effects on bone suggested that GTP may serve as an effective dietary supplement to prevent osteoporosis in patients with low bone mass. It is worthy to point out that even though green tea and its metabolites are found to be useful in treating bone loss, there is still a gap in our knowledge that needs to be filled in regard to the translation of findings in animal observations and how this is applied to human populations. Evidence from all animal studies only shows an increase in BMD without testing bone strength and anti-fracture capacity; these animal data mainly focus on long bones, whereas the published human data are for spine and hip. In addition, there are still limited data supporting the BMD increment and anti-fracture effect of green tea from longitudinal studies. In future human studies, green tea and its active ingredients should be given for long-term periods, the bioavailability should be monitored via validated biomarkers, and efficacy in terms of bone mass and microarchitecture should be evaluated through advanced imaging technology to ensure their possible ben-

References

[1] Bao Q, Pan J, Qi H, Wang L, Qian H, Jiang F, Shao Z, Xu F, Tao Z, Ma Q, Nelson P, Hu X. Aging and age-related diseases-from endocrine therapy to target therapy. Mol Cell Endocrinol 2014; 394: 115-118.
[2] Guarente L. Aging research-where do we stand and where are we going? Cell 2014; 159: 15-19.
[3] Harman D. Aging: a theory based on free radical and radiation chemistry. J Gerontol 1956; 11: 298-300.

[4] Harman D. The aging process. Proc Natl Acad Sci U S A 1981; 78: 7124-7128.

[5] De Magalhaes JP, Church GM. Cells discover fire: employing reactive oxygen species in development and consequences for aging. Exp Gerontol 2006; 41: 1-10.

[6] Djamali A. Oxidative stress as a common pathway to chronic tubulointerstitial injury in kidney allografts. Am J Physiol Renal Physiol 2007; 293: F445-455.

[7] NIH Consensus Development Panel on Osteoporosis Prevention, Diagnosis, and Therapy. Osteoporosis prevention, diagnosis, and therapy. JAMA 2001; 285: 785-795.

[8] Holroyd C, Cooper C, Dennison E. Epidemiology of osteoporosis. Best Pract Res Clin Endocrinol Metab 2008; 22: 671-685.

[9] Boonen S, Dejaeger E, Vanderschueren D, Venken K, Bogaerts A, Verschueren S, Milisen K. Osteoporosis and osteoporotic fracture occurrence and prevention in the elderly: a geriatric perspective. Best Pract Res Clin Endocrinol Metab 2008; 22: 765-785.

[10] Burge R, Dawson-Hughes B, Solomon DH, Wong JB, King A, Tosteson A. Incidence and economic burden of osteoporosis-related fractures in the United States, 2005-2025. J Bone Miner Res 2007; 22: 465-475.

[11] Park IK, Qian D, Kiel M, Park IK, Qian D, Kiel M, Becker MW, Pihalja M, Weissman IL, Morrison SJ, Clarke MF. Bmi-1 is required for maintenance of adult self-renewing haematopoietic stem cells. Nature 2003; 423: 302-305.

[12] Jin J, Lv X, Chen L, Zhang W, Li J, Wang Q, Wang R, Lu X, Miao D. Bmi-1 plays a critical role in protection from renal tubulointerstitial injury by maintaining redox balance. Aging Cell 2014; 13: 797-809.

[13] Zhang HW, Ding J, Jin JL, Guo J, Liu JN, Karaplis A, Goltzman D, Miao D. Defects in mesenchymal stem cell self-renewal and cell fate determination lead to an osteopenic phenotype in Bmi-1 null mice. J Bone Miner Res 2010; 25: 640-652.

[14] Liu J, Cao L, Chen J, Song S, Lee IH, Quijano C, Liu H, Keyvanfar K, Chen H, Cao LY, Ahn BH, Kumar NG, Rovira II, Xu XL, van Lohuizen M, Motoyama N, Deng CX, Finkel T. Bmi1 regulates mitochondrial function and the DNA damage response pathway. Nature 2009; 459: 387-392.

[15] Food and Agriculture Organization of the United Nations-Production FAOSTAT. Medium-term prospects for agricultural commodities. Available from: http://www.fao.org/docrep/ 006/y5143e/y5143e00.htm (cited 10 August 2010).

[16] Balentine DA, Wiseman SA, Bouwens LC. The chemistry of tea fla-vonoids. Crit Rev Food Sci Nutr 1997; 37: 693-704.

[17] Oka Y, Iwai S, Amano H, Irie Y, Yatomi K, Ryu K, Yamada S, Inagaki K, Oguchi K. Tea polyphenols inhibit rat osteoclast formation and differentiation. J Pharmacol Sci 2012; 118: 55-64.

[18] Yang CS, Landau JM. Effects of tea consumption on nutrition and health. J Nutr 2000; 130: 2409-2412.

[19] Nakagawa H, Wachi M, Woo JT, Kato M, Kasai S, Takahashi F, Lee IS, Nagai K. Fenton reaction is primarily involved in a mechanism of (-)-epigallocatechin-3-gallate to induce osteoclastic cell death. Biochem Biophys Res Commun 2002; 292: 94-1012.

[20] Hafeez BB, Ahmed S, Wang N, Gupta S, Zhang A, Haqqi TM. Green tea polyphenols-induced apoptosis in human osteosarcoma SAOS-2 cells involves a caspase-dependent mechanism with downregulation of nuclear factor-kappaB. Toxicol Appl Pharmacol 2006; 216: 11-19.

[21] Yun JH, Pang EK, Kim CS, Yoo YJ, Cho KS, Chai JK, Kim CK, Choi SH. Inhibitory effects of green tea polyphenol (-)-epigallocatechin gallate on the expression of matrix metalloproteinase-9 and on the formation of osteoclasts. J Periodontal Res 2004; 39: 300-307.

[22] Tokuda H, Takai S, Hanai Y, Matsushima-Nishiwaki R, Hosoi T, Harada A, Ohta T, Kozawa O. (-)-Epigallocatechin gallate suppresses endothelin-1-induced interleukin-6 synthesis in osteoblasts: inhibition of p44/p42 MAP kinase activation. FEBS Lett 2007; 581: 1311-1316.

[23] Tokuda H, Takai S, Matsushima-Nishiwaki R, Akamatsu S, Hanai Y, Osoi T, Harada A, Ohta T, Kozawa O. (−)-Epigallocatechin gallate enhances prostaglandin F2 alpha-induced VEGF synthesis via upregulating SAPK/JNK activation in osteoblasts. J Cell Biochem 2007; 100: 1146-1153.

[24] Morinobu A, Biao W, Tanaka S, Horiuchi M, Jun L, Tsuji G, Sakai Y, Kurosaka M, Kumagai S. (-)-Epigallocatechin-3-gallate suppresses osteoclast differentiation and ameliorates experimental arthritis in mice. Arthritis Rheum 2008; 58: 2012-2018.

[25] Lee JH, Jin H, Shim HE, Kim HN, Ha H, Lee ZH. Epigallocatechin-3-gallate inhibits osteoclastogenesis by down-regulating c-Fos expression and sup-pressing the nuclear factor-kappaB signal. Mol Pharmacol 2010; 77: 17-25.

[26] Lin RW, Chen CH, Wang YH, Ho ML, Hung SH, Chen IS, Wang GJ. (-)-Epigallocatechin gallate inhibition of osteoclastic differentiation via NF-kappaB. Biochem Biophys Res Commun 2009; 379: 1033-1037.

[27] Cao G, Gu M, Zhu M, Gao J, Yin Y, Marshall C, Xiao M, Ding J, Miao D. Bmi-1 absence causes premature brain degeneration. PLoS One 2012; 7: e32015.

[28] Shen CL, Yeh JK, Cao JJ, Wang JS. Green tea and bone metabolism. Nutr Res 2009; 29: 437-456.

[29] Miao D, Bai X, Panda D, McKee M, Karaplis A, Goltzman D. Osteomalacia in hyp mice is associated with abnormal phex expression and with altered bone matrix protein expression and deposition. Endocrinology 2001; 142: 926-939.

[30] Panda DK, Miao D, Bolivar I, Li J, Huo R, Hendy GN, Goltzman D. Inactivation of the 25-hydroxyvitamin D 1alpha-hydroxylase and vitamin D receptor demonstrates independent and interdependent effects of calcium and vitamin D on skeletal and mineral homeostasis. J Biol Chem 2004; 279: 16754-16766.

[31] Miao D and Scutt A. Histochemical localization of alkaline phosphatase activity in decalcified bone and cartilage. J Histochem Cytochem 2002; 50: 333-340.

[32] Miao D and Scutt A. Recruitment, augmentation and apoptosis of rat osteoclasts in 1,25-(OH)2D3 response to short-term treatment with 1,25-dihydroxyvitamin D3 in vivo. BMC Musculoskelet Disord 2002; 3: 16.

[33] Jin J, Zhao Y, Tan X, Guo C, Yang Z, Miao D. An improved transplantation strategy for mouse mesenchymal stem cells in an acute myocardial infarction model. PLoS One 2011; 6: e21005.

[34] Liu J, Lv F, Sun W, Tao C, Ding G, Karaplis A, Brown E, Goltzman D, Miao D. The abnormal phenotypes of cartilage and bone in calcium-sensing receptor deficient mice are dependent on the actions of calcium, phosphorus, and PTH. PLoS Genet 2011; 7: e1002294.

[35] Xue Y, Karaplis AC, Hendy GN, Goltzman D, Miao D. Genetic models show that parathyroid hormone and 1,25-dihydroxyvitamin D3 play distinct and synergistic roles in post-natal mineral ion homeostasis and skele-tal development. Hum Mol Genet 2005; 14: 1515-1528.

[36] Nijweide PJ, Burger EH, Feyen JH. Cells of bone: proliferation, differentiation, and hormonal regulation. Physiol Rev 1986; 66: 855-886.

[37] Ando K, Mori K, Rédini F, Heymann D. RANKL/RANK/OPG: key therapeutic target in bone oncology. Curr Drug Discov Technol 2008; 5: 263-268.

[38] Matsuo K, Irie N. Osteoclast-osteoblast communication. Arch Biochem Biophys 2008; 473: 201-209.

[39] Suda T, Takahashi N, Martin TJ. Modulation of osteoclast differentiation. Endocr Rev 1992; 13: 66-80.

[40] Steinbeck MJ, Appel WH Jr, Verhoeven AJ, Karnovsky MJ. NADPH-oxidase expression and in situ production of superoxide by osteoclasts actively resorbing bone. J Cell Biol 1994; 126: 765-772.

[41] Darden AG, Ries WL, Wolf WC, Rodriguiz RM, Key LL Jr. Osteoclastic superoxide production and bone resorption: stimulation and inhibition by modulators of NADPH oxidase. J Bone Miner Res 1996; 11: 671-675.

[42] Yavropoulou MP, Yovos JG. Osteoclastogenesis-current knowledge and future perspectives. J Musculoskelet Neuronal Interact 2008; 8: 204-216.

[43] Fazzalari NL. Bone remodeling: a review of the bone microenviron-ment perspective for fragility fracture (osteoporosis) of the hip. Semin Cell Dev Biol 2008; 19: 467-472.

[44] Banfi G, Iorio EL, Corsi MM. Oxidative stress, free radicals and bone remodeling. Clin Chem Lab Med 2008; 46: 1550-1555.

[45] Manolagas SC. De-fense! De-fense! De-fense: scavenging H2O2 while making cholesterol. Endocrinology 2008; 149: 3264-3266.

[46] Mody N, Parhami F, Saraflan TA, Demer LL. Oxidative stress modulates osteoblastic differentiation of vascular and bone cells. Free Radic Biol Med 2001; 31: 509-519.

[47] Shen CL, Wang P, Guerrieri J, Yeh J, Wang JS. Protective effect of green tea polyphenols on bone loss in middle-aged female rats. Osteoporosis Int 2008; 19: 979-990.

[48] Fatokun AA, Stone TW, Smith RA. Responses of differentiated MC3T3-E1 osteoblast-like cells to reactive oxygen species. Eur J Pharmacol 2008; 587: 35-41.

[49] Bai XC, Lu D, Bai J, Zheng H, Ke ZY, Li XM, Luo SQ. Oxidative stress inhibits osteoblastic differentiation of bone cells by ERK and NF-κB. Biochem Biophys Res Commun 2004; 314: 197-207.

[50] Dreher I, Schütze N, Baur A, Hesse K, Schneider D, Köhrle J, Jakob F. Selenoproteins are expressed in fetal human osteoblast-like cells. Biochem Biophys Res Commun 1998; 245: 101-107.

[51] Fuller K, Lean JM, Bayley KE, Wani MR, Chambers TJ. A role for TGF-βin osteoclast differentiation and survival. J Cell Sci 2000; 113: 2445-2453.

[52] Yang S, Madyastha P, Bingel S, Ries W, Key L. A new superoxide-generating oxidase in murine osteoclasts. J Biol Chem 2001; 276: 5452-5458.

[53] Sontakke AN, Tare RS. A duality in the roles of reactive oxygen species with respect to bone metabolism. Clin Chim Acta 2002; 318: 145-148.

[54] Garrett JR, Boyce BF, Oreffo RO, Bonewald L, Poser J, Mundy GR. Oxygen-derived free radicals stimulate osteoclastic bone resorption in rodent bone in vitro and in vivo. J Clin Invest 1990; 85: 632-639.